Fire and Ice

Volcanism and the Ice-Albedo Feedback

E. Giroud-Proeschel - 52917770
P. Matlashewski - 45701109
M. Ormerod - 16265167

November 20, 2020

Word Count: 2456

Contents

1 Introduction

Earth's past is marked by extreme climate variations, with evidence of reversals between hothouse and coldhouse regimes. A possible driving force behind these reversals is volcanism. In this study, we focus on how large volcanic out-gassing of volatiles such as sulfur dioxide, affect the Earth's climate. Here we chose to investigate the impact of volcanic perturbations on a simple radiative energy balance model. Throughout this paper we will only consider the effect of aerosols, and more specifically, SO2. This model is inspired by the work of Russian climatologist Mikhail I. Budyko, who discovered the ice-albedo feedback mechanism through his pioneering of studies on global climate using physical models of temperature equilibrium (Budyko 1969). We proceed as follows:

1. Build a graphical algorithm solving the radiative energy balance equations in a zonally-averaged Earth model (section 5.2).

2. Compute a steady-state energy balance of the Earth to investigate the effects of inter-zonal transfer by:

   (a) setting all transfer coefficients k_{ij} to zero and finding the equilibrium temperature distribution.

   (b) using the provided values of k_{ij} and comparing heat transfer magnitudes and rates from our previous step.

3. To investigate the cooling effects of volcanism, we use data from the 1982 El Chichón and Pinatubo eruptions (Robock 2000) to characterize the spatially and temporally reducing effects of stratospheric aerosols on incoming solar radiation.

4. To parameterize the intensity volcanic cooling, we model the frequency of volcanic eruptions as a Poisson process.

5. To consider the possibility of a coldhouse regime (or snowball Earth), we introduce an ice-albedo feedback using temperature-dependent zonal albedos.

6. Finally, we combine the cooling effects of volcanism combined with the ice-albedo feedback model to investigate if volcanic activity can give rise to a snowball Earth scenario.

1.1 Budyko Climate Model

The evolution of Earth's temperature will be investigated using a Budyko climate model (Budyko 1969). The earth is divided into 6 latitudinal zones, defined in table 1 and figure 1 (Jellinek 2020).

Zone	Lower Latitude	Upper Latitude
1	$90°S$	$60°S$
2	$60°S$	$30°S$
3	$30°S$	$0°$
4	$0°$	$30°N$
5	$30°S$	$60°N$
6	$60°S$	$90°N$

Table 1: Zone latitudes.

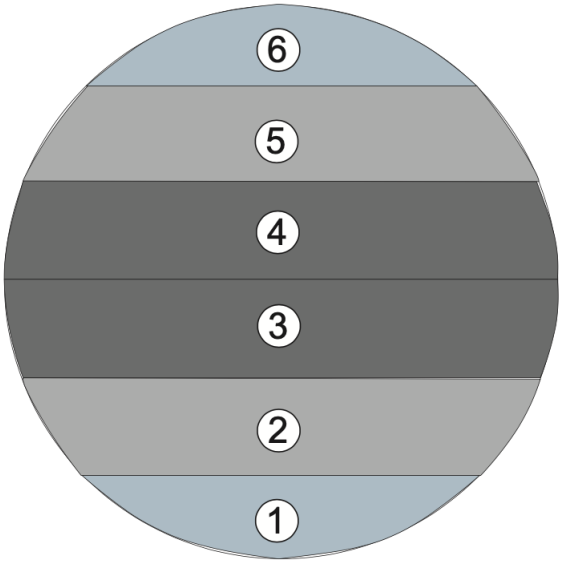

Figure 1: Latitude zone intervals.

Within each zone, temperature evolves through a balance of incoming solar radiation, outgoing long-wave radiation and the exchange of heat between zones. These effects are quantified through

$$\frac{dT_k}{dt} = \frac{1}{\overline{\rho_k c_k[Z_k]}}\{\gamma_k(1-\alpha_k^{sky})(1-\bar{\alpha}_k)S_0 - \tau\sigma_B T_k^4\} + \frac{L_{ki}k_{ki}}{A_k\overline{\rho_k c_k[Z_k]}}(T_k - T_i) \tag{1}$$

where $k = 1, \ldots, 6$ represents each latitudinal zone and T_k is the zonal temperature. The remaining constants are defined in tables 9 and 10 of section 5.3.2.

1.2 Volcanic Eruptions

Volcanism is an important natural cause of climate change on both short and long-term timescales (Robock 2000). For our investigation, we consider the short-term cooling effects of volcanism that occur on a $10 - 100$ year time frame. A zonal occlusion factor, $\phi_k(t)$, introduces this cooling effect to our model (equation 2). The occlusion factor represents

volcanic aerosols suspended in the atmosphere that block direct shortwave solar radiation.

$$\frac{dT_k}{dt} = \frac{1}{\rho_k c_k [Z_k]}\{\phi_k(t)\gamma_k(1-\alpha_k^{sky})(1-\bar{\alpha}_k)S_0 - \tau\sigma_B T_k^4\} + \frac{L_{ki}k_{ki}}{A_k\rho_k c_k [Z_k]}(T_k - T_i) \qquad (2)$$

A value of $\phi(t) = 1$ represents no volcanic aerosol occlusion. A value of $\phi(t) = 0.7$, for example, represents a 30% reduction in total incoming solar radiation.

1.2.1 Direct Radiation Occlusion

The function $\phi(t)$ was fit to observations of reduced solar radiation following the 1982 El Chichón eruption and the 1991 Pinatubo eruption (Robock 2000) (figure 2). We found that a function with the form $\phi(t) = 1 - ct^{-2}$, where $c = 5.36$ yr^2 is an empirical constant found through nonlinear regression, gave a reasonable representation of the data. This function has the property that $\phi(t) \to 1$ as $t \to \infty$, which models the decaying effects of aerosol occlusion over time.

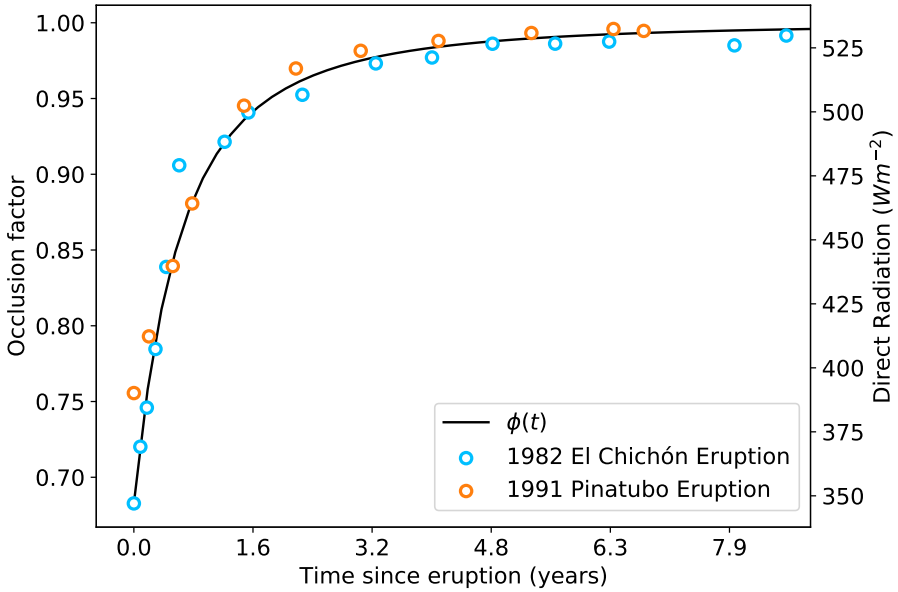

Figure 2: A plot of the empirically fit occlusion function.

1.2.2 Spatial Distribution of Aerosols

The effects of a volcanic eruption are not restricted to a single zone. Suspended aerosols are dispersed throughout the atmosphere and can travel large distances across the Earth. To model the spatial effects of aerosol dispersion following an eruption, a time lag is introduced to the zonal occlusion functions, $\phi_k(t)$, that varies based on the distance zone k is from the eruption zone. An example is shown in figure 3, where an eruption occurs at $t = 0$ in zone 1. For the first 3 months following the eruption, only zone 1 has the occluding effects of volcanic aerosols. After 3 months, the aerosols have traveled to the adjacent zone 2, where $\phi_2(t)$ begins to follow the decaying occlusion function defined in section 1.2.1. Global coverage occurs

after approximately 9 months. The specific lag times considered were estimated from the data presented in Robock 2000.

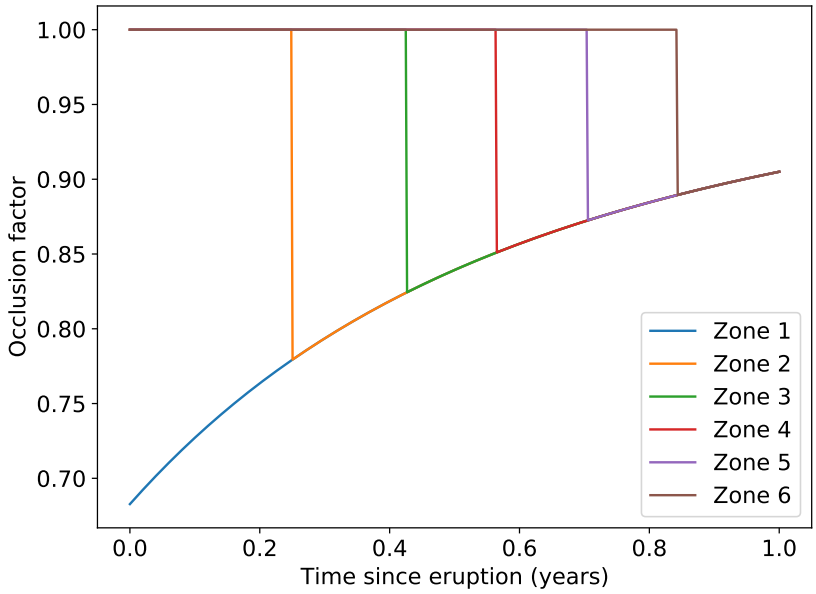

Figure 3: The spatial effect of eruptions. A distance-dependent time lag is present for zones adjacent to the eruption.

1.2.3 Stochastic Eruption Frequency

Sections 1.2.1 and 1.2.2 define our model's response to a single eruption. To investigate the intensity of volcanism on the Earth's climate, we allow for a series of eruptions to occur over time. Volcanic eruptions in each zone are modeled as a Poisson process, where each zone is prescribed an eruption frequency parameter, λ_k, reflecting the average repose time between eruptions in the zone. For an eruption frequency λ_k, the probability of a repose time, t_R, between eruptions follows an exponential distribution

$$P(t_R) = \lambda_k e^{-\lambda_k t_R} \tag{3}$$

For this investigation, we assume eruptions occur independently between zones.

The intensity of volcanic activity on Earth can be adjusted through λ_k. A smaller λ_k represents shorter repose times and higher volcanic activity. Combining equation 3 with the occlusion function defined in sections 1.2.1 and 1.2.2 gives a simple stochastic model for volcanism on Earth that includes the time-decaying effects of aerosol occlusion, the spatial dispersion of aerosols and eruption frequency.

1.3 Ice-Albedo Feedback

The volcanism defined in section 1.2 provides a mechanism to cool the Earth by occluding direct solar radiation with suspended volcanic aerosols. One interesting way to study the

implications of this cooling is by considering the ice-albedo feedback (Budyko 1969). If the temperature of the Earth is cold enough, ice will grow and cover a larger proportion of the Earth's surface. This will result in a higher surface albedo, reflecting more incoming solar radiation. This further contributes decreasing the temperature of the Earth, leading to a positive feedback and a potential "snowball Earth" scenario.

Ice-albedo feedback is modeled by defining a temperature dependent albedo as follows

$$\alpha_k(T_k) = \begin{cases} \alpha_{k0} & T_k \geq T_0 \\ \alpha_{k0} + (\alpha_i - \alpha_k)\frac{(T_k - T_0)^2}{(T_i - T_0)^2} & T_i < T_k < T_0 \\ \alpha_i & T_k \leq T_i \end{cases} \tag{4}$$

where α_k is the albedo in zone k, T_k is the temperature in zone k, $T_0 = 280$ K is the threshold temperature below which zonal ice cover will grow to increase the albedo, $T_i = 250$ K is the temperature where the zone is completely covered in ice, α_{k0} is the baseline zonal albedo given in table 9 and $\alpha_i = 0.6$ is the albedo of ice. Figure 4 shows the nonlinear albedo function for each zone.

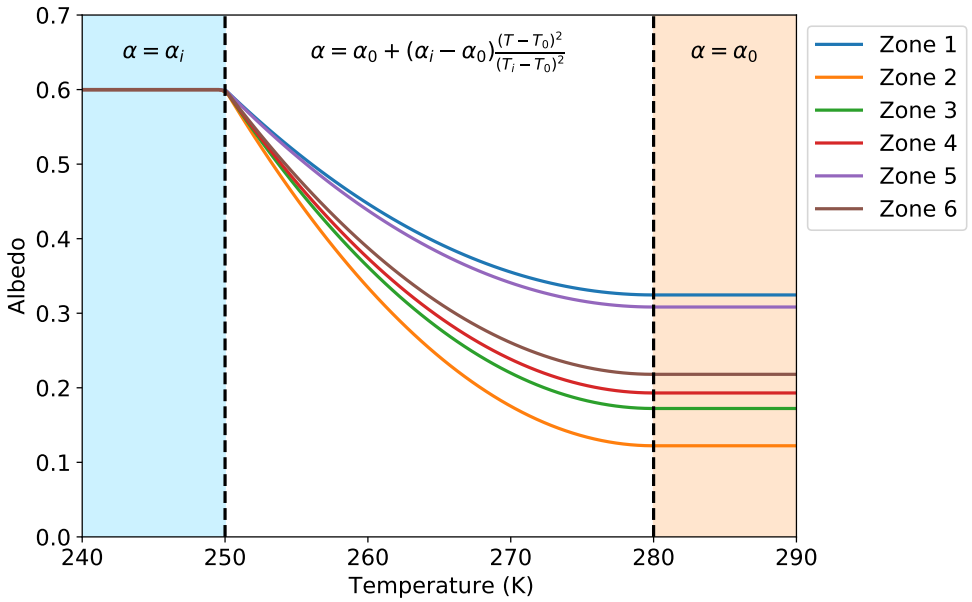

Figure 4: Albedo parameterization as a function of temperature in each zone. The blue shaded region indicates the temperature range where a zone is covered with ice. The orange shaded region indicates the temperature range where there is no change in ice as temperature varies.

2 Results

2.1 Steady-State Climate Model: No Volcanism

By passing initial condition temperatures calculated through our model with suppressed inter-zonal transfer (table 2) to our model where inter-zonal transfer is allowed. Figure 5

shows the equilibrium temperatures for a model where El Niño is neglected (dashed lines) and where El Niño is considered (solid lines).

Zone	Inter-zonal Heat Transfer Suppressed Equilibrium Temperature [K]	Inter-zonal Heat Transfer Allowed Equilibrium Temperature [K]
1	217.23	274.12
2	279.74	279.34
3	296.45	282.26
4	294.56	280.88
5	263.56	279.71
6	225.33	274.93

Table 2: Equilibrium Temperature distributions for a climate model with no volcanism

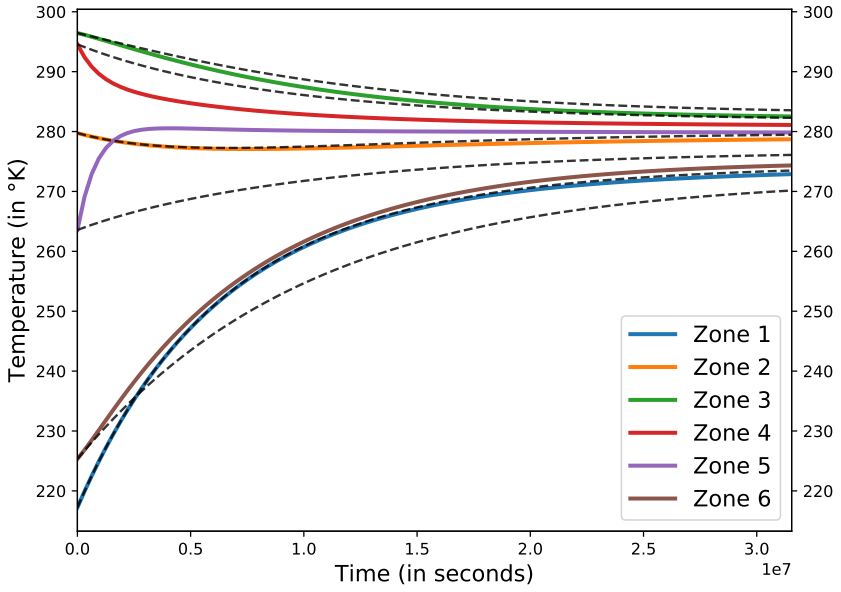

Figure 5: Equilibrium solution for 6-zoned Earth climate model. Zone 1 marks the southernmost band at $60 - 90°$S while zone 6 represents the northernmost band at $60 - 90°$N. Zones 2-5 are bands covering $30°$ intervals between zones 1 and 6 (See Figure 1).

2.2 Climate Model Following Single Volcanic Eruption

Figure 6 shows the effect of a single eruption on zonal temperatures initially at steady-state. The eruption occurs in zone 4 after 1 year, as indicated by the vertical dashed line. Zone 4 is immediately affected by the solar occlusion and shows a decrease in temperature. A time lag between the zonal temperature responses is clearly visible with zones at a greater

distance from zone 4 showing a larger time lag. The recovery of each zone to its equilibrium temperature occurs over approximately 15 years after the eruption. The equilibrium temperature values are the same post-eruption as they are pre-eruption.

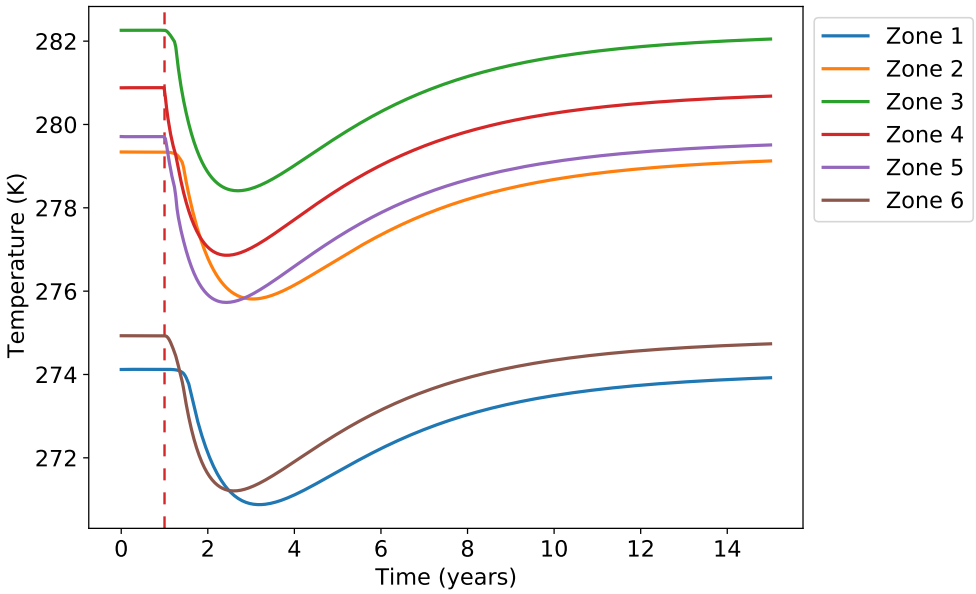

Figure 6: Reduction in solar forcing post eruption results in temperature drop.

2.3 Stochastic Volcanic Eruptions

Figure 7 shows a model result that includes multiple eruptions following the Poisson process defined in section 1.2.3. Vertical dashed lines represent an eruption with a coloured by the zone the eruption occurred. The eruption intensity parameters used are given in table 3

Zone	$\lambda_k[\mathrm{yr}^{-1}]$
1	100
2	50
3	20
4	20
5	50
6	100

Table 3: Volcanic intensity rate parameters

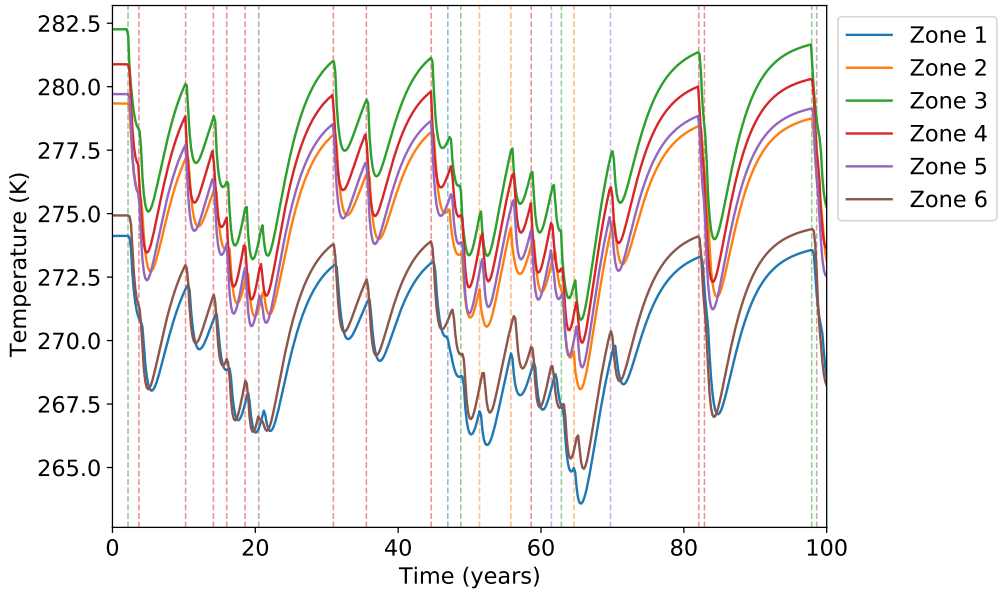

Figure 7: Stochastic eruption distribution following Poisson distribution. Vertical dotted lines are colored based on the zone the eruption occurred in, and their placement is the point in time at which the eruption is initiated.

The model was run for 100 years to show multiple cycles of temperature drops and recoveries. From Figure 7, we see that following each eruption is a decline in zonal temperatures, and sufficiently close eruptions, in time, compound that effect. The distribution lag associated with aerosol spreading is still represented numerically, though a lag of a few months is difficult to discern visually on this extended time scale.

2.4 The Ice-Albedo Effect

Figure 8 shows the result of the temperature dependent albedo from in equation 4 coupled with our climate model in equation 1. The temperature ranges for the nonlinear albedo model are coloured similar to figure 4. We recognize three temperature equilibria, two of which are stable and one that is unstable. The equilibrium temperature distributions are shown in table 4.

Zone	Warm Earth Equilibrium Temperature [K]	Unstable Equilibrium Temperature [K]	Snowball Earth Equilibrium Temperature [K]
1	274.02	251.08	231.91
2	279.27	255.03	234.30
3	282.21	258.31	236.23
4	280.83	257.78	236.13
5	279.66	256.98	235.70
6	274.83	253.11	233.20

Table 4: Ice-albedo effect equilibrium temperature distributions

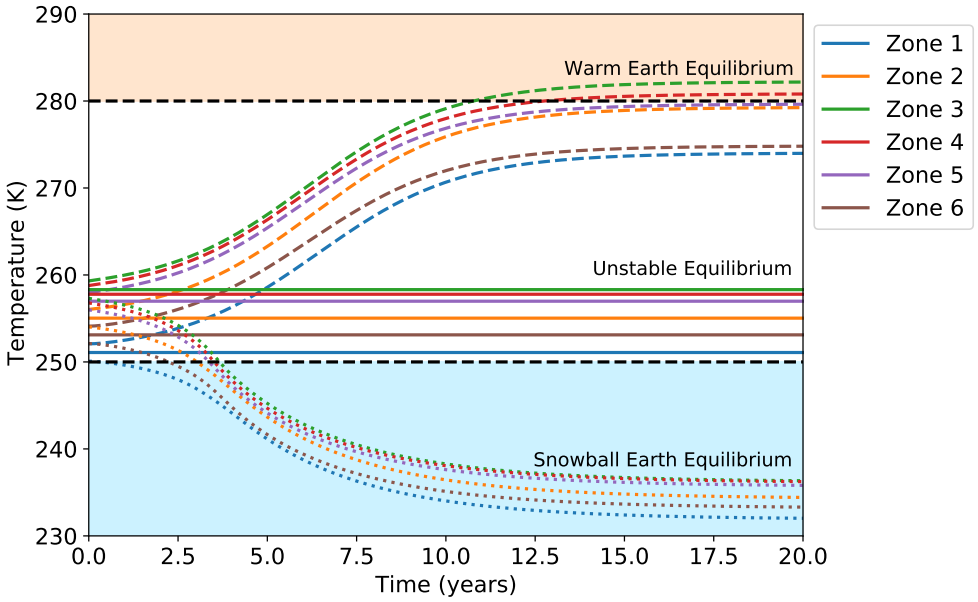

Figure 8: Integrating through climate model incorporating both stochastic volcanic eruptions and ice-albedo feedback parameterization.

A model started with an initial temperature distribution at the unstable equilibrium (solid lines in figure 8) remains at the unstable equilibrium.

A model started with an initial temperature distribution perturbed slightly above the unstable equilibrium (dashed lines in figure 8) asymptotically approaches the "warm Earth" equilibrium given in table 4.

A model started with an initial temperature distribution perturbed slightly below the unstable equilibrium (dotted lines in figure 8) asymptotically approaches the "snowball Earth" equilibrium given in table 4. The temperature difference between high-latitudinal and mid-latitudinal zones is much smaller for the snowball Earth equilibrium compared to the warm Earth equilibrium.

There is a slight decrease in equilibrium temperatures for the warm Earth equilibrium when compared to the equilibrium for the model with no ice-albedo feedback (as shown in tables 2 and 4) due to some of the equilibrium temperatures falling in the variable albedo range.

2.5 Fire and Ice: Stochastic Volcanism and the Ice-Albedo Feedback

Figure 9 shows the results of two models that combine volcanism defined in section 1.2 with the ice-albedo feedback defined in section 1.3. The temperature ranges for the nonlinear albedo model are coloured similar to figure 4. The "Stable Eruption Frequency"

Zone	Stable Eruption Frequency $\lambda_k[\text{yr}^{-1}]$	Unstable Eruption Frequency $\lambda_k[\text{yr}^{-1}]$
1	150	100
2	75	50
3	50	20
4	50	20
5	75	50
6	150	100

Table 5: Volcanic intensity rate parameters for the volcanism with ice-albedo feedback models

and "Unstable Eruption Frequency" models were forced with the eruption intensity rate parameters shown in table 5.

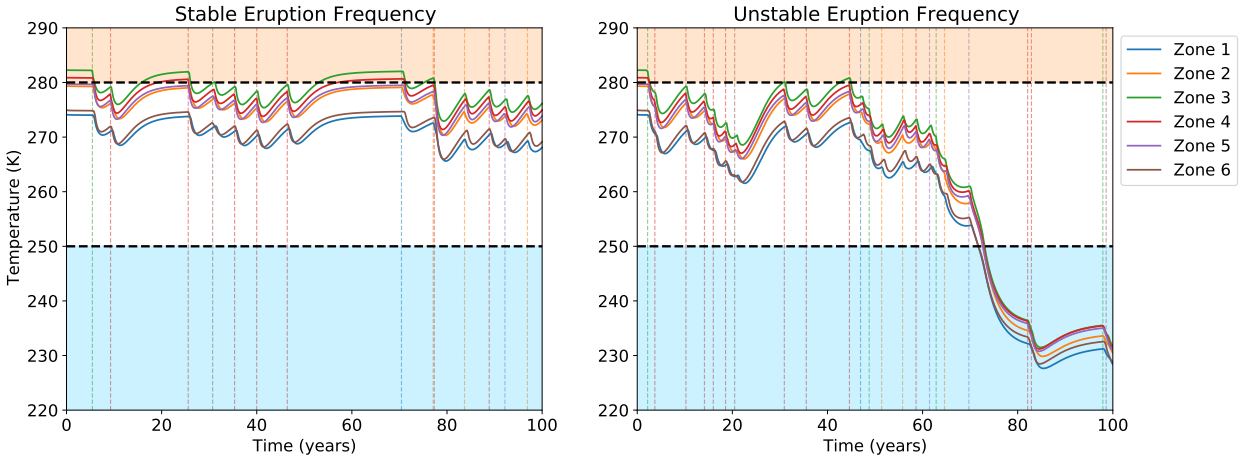

Figure 9: Model results for volcanism combined with the ice-albedo feedback.

The stable eruption frequency model oscillates around the warm Earth equilibrium shown in section 2.4. The unstable eruption frequency oscillates around the warm Earth equilibrium for approximately 70 years before it quickly drops to oscillate around the snowball Earth equilibrium.

3 Discussion

3.1 Steady-State Climate Model: No Volcanism

The El Niño phenomena increases the rate of atmospheric and ocean heat exchange allowing zonal temperatures to approach equilibrium more quickly.

3.2 Volcanic Eruptions

One of the aims of our study was to investigate the short-term impact of volcanism on Earth's climate. The occlusion factor introduced in section 1.2.1 ultimately acts to cool the

climate by blocking direct solar radiation from reaching the Earth's surface.

An interesting result is the difference in time scales for the occluding effect of an eruption and the subsequent recovery time of the temperature. Figure 2 shows that suspended aerosols block less than 5% of direct solar radiation 2 years after an eruption. On the other hand, figure 6 shows that it takes over a decade before zonal temperatures recover to within 5% of their equilibrium. This demonstrates volcanic aerosols have an impact on the radiative energy balance of the Earth, even after the aerosols have dissipated and are no longer blocking direct solar radiation.

The longer recovery time increases the susceptibility of the climate to compounding temperature drops from multiple eruptions, as see in figure 7. Temperatures are forced to values over 10 degrees below their equilibrium values during intense volcanic episodes. These high intensity volcanic episodes can be a trigger that drives to Earth away from its initial equilibrium into a snowball Earth state.

3.3 The Ice-Albedo Effect

The nonlinear albedo dependence on temperature defined in equation 4 ultimately gives rise to three equilibrium conditions, as illustrated in figure 8. The "warm Earth" equilibrium represents conditions where the ice-albedo feedback has a small effect on the Earth's global energy balance. Even when temperatures fall in the variable albedo temperature range (i.e. $250\text{K} < T < 280\text{K}$), no ice-albedo runaway is observed.

The "snowball Earth" equilibrium represents conditions where the ice-albedo feedback has forced the Earth into a uniform, ice-covered state where each zone has the characteristic albedo of ice.

Small changes in temperature near either of these equilibria are compensated by a change in heat flow from adjacent zones as well as a net imbalance of radiative energy fluxes which restores the temperatures to equilibrium.

The presence of two stable equilibria implies the existence of a third, unstable equilibrium that separates the stable warm Earth and snowball Earth temperature regimes. This unstable equilibrium arises as a consequence of the nonlinear albedo dependence on temperature. A decrease in temperature near the unstable equilibrium results in a sufficiently high increase in albedo where the reflected solar radiation drives temperatures lower and further increases the albedo, resulting in a positive feedback.

For a snowball Earth, the zonal albedo is constant, resulting a narrower distribution of equilibrium temperatures. However, the higher heat transfer coefficient between zones 4 and 5 maintains distinct equilibrium temperatures for every zone.

3.4 Fire and Ice: Stochastic Volcanism and the Ice-Albedo Feedback

Combining the cooling effects of volcanism with the ice-albedo feedback gives a mechanism for driving the Earth away from its baseline, warm equilibrium. We found that the Earth's temperatures are able to recover towards the warm Earth equilibrium as long as volcanic eruption frequency is low enough (represented by long repose times). If volcanic eruption frequency is high enough (short repose times), the Earth's temperatures drop below the critical unstable equilibrium temperatures, and the runaway ice-albedo feedback drives the model to the snowball Earth equilibrium (figure 9).

3.5 Model Limitations

The Budyko climate model considered in this investigation greatly simplifies the mechanics of heat exchange between latitudinal zones. In addition to the inherent limitations of treating latitudinal heat exchange with constant conductivity coefficients, a number of simplifications were made in our parameterization of volcanic eruptions.

The most important limitation is the absence of the heating effects of volcanism. CO_2 is a significant component of volcanic emissions and is a strong greenhouse gas. When present in the atmosphere, CO_2 re-emits outgoing long-wave radiation back to the Earth's surface. This ultimately reduces the total outgoing radiation from the Earth, resulting an increase in surface temperature.

As such, the accumulation of greenhouse gasses from volcanic eruptions may provide a means to return to a warm Earth equilibrium by increasing surface temperatures above the critical temperature threshold identified in our study.

Another limitation of our volcanic model is the assumption of a single eruption type. A model that allows for a variation in eruption intensity and composition would provide finer grain control over an eruption's impact the atmosphere and its subsequent effects on Earth's surface temperatures.

We required an arbitrary increase in eruption rate frequencies to drive the Earth to a snowball equilibrium. This is a consequence of modelling eruptions as a stationary Poisson process. A non-stationary stochastic model of eruptions could allow for the clustering of eruption activity as an alternative mechanism to trigger the runaway ice-albedo feedback.

A limitation of our ice-albedo model is that as ice cover increases with dropping temperatures, there may be an impact on atmospheric and oceanic heat circulation. Our model does not parameterize these effects. For example, the heat transfer coefficient, k_{45}, representing the El Niño phenomena in our model is constant, though this value is likely dependent on the changing ocean and atmospheric interactions.

4 Conclusion

Inter-zonal heat transfer coefficients dictate the rate and efficiency of heat distribution in our model. By implementing a stochastic eruption frequency distribution as well as a nonlinear relationship between temperature and albedo, we characterized the effect of volcanic activity on the global energy balance. We found three equilibrium solutions, one being the snowball Earth state, which can be approached through volcanism-induced temperature perturbations. Our model parametrization, however, didn't allow an escape from this new stable state.

4.1 Future Work

As discussed in section 3.5, there are a number of ways our model can be extended to consider different aspects of volcanism and its coupling with ice-albedo feedback. A particularly interesting future direction to consider would be the inclusion of the warming effect of volcano greenhouse gases. In this way, volcanism can be studied as both a driving force to push Earth into a snowball equilibrium as well as a way to recover from a snowball equilibrium.

5 Ancillary Information

5.1 Author Contributions

Section	Subsection	Contributors
Graphic	Box-Model	M
Code	Steady-State Climate	P and E
Code	Perturbation: Single Volcanic Eruption	P, E, and M
Code	Snowball Earth	P, E, and M
Introduction	Motivation	E and M
Introduction	Budyko Climate Model	P
Introduction	Direct Radiation Occlusion	P
Introduction	Spatial Distribution of Aerosols	P
Introduction	Ice-albedo Feedback	P
Results	Steady-State Climate	M
Results	Perturbation: Single Volcanic Eruption	M, E, P
Results	Fire and Ice	M and P
Discussion	Steady-State Climate Model	M
Discussion	Perturbation: Single Volcanic Eruption	P
Discussion	Fire and Ice	E, P, M
Discussion	Model Limitations	E, P, M
Conclusion	Future Work	E, M, and P
Conclusion	Summary	E, M, and P

Table 6: Contributions does not necessarily reflect discussion and preparation behind concepts as this required continuous lateral communication between authors. For example, all discussion sections were analyzed with input from each author, but written by

5.2 Algorithm Development

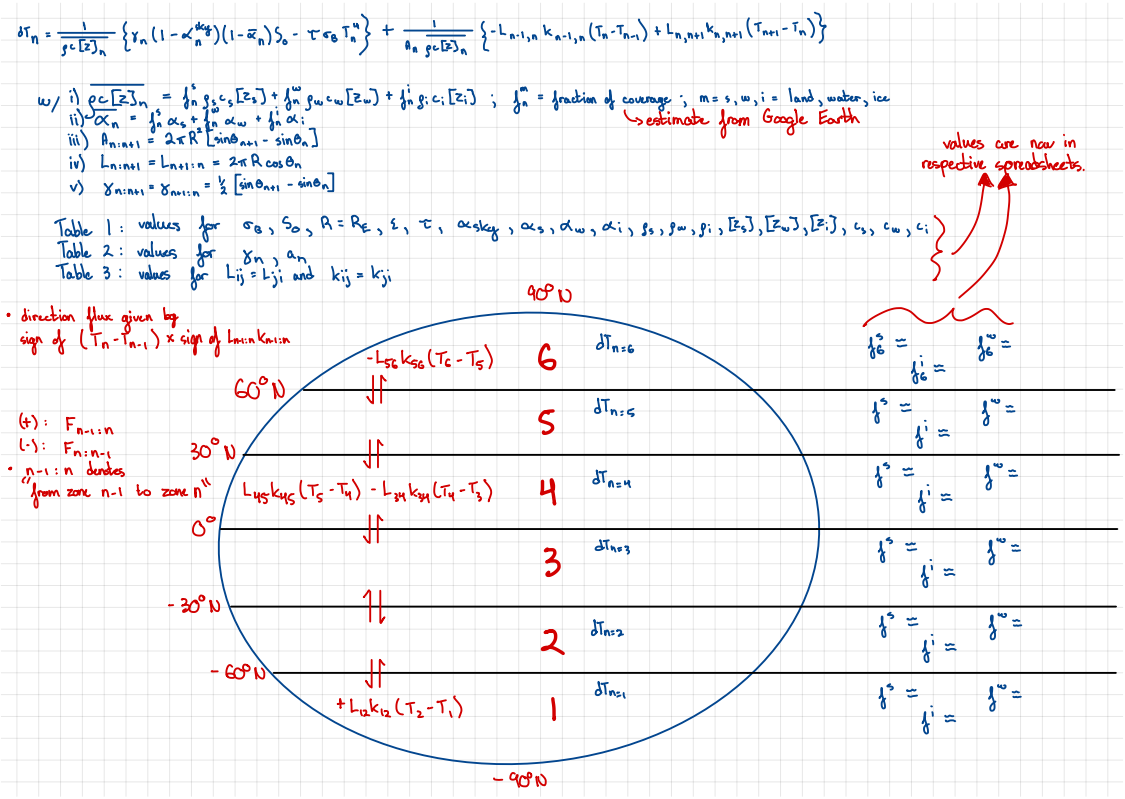

Figure 10: Sketch depicting zone intervals and necessary parameters for numerical solving.

5.3 Data

5.3.1 Eruption Times Series

Table 7: Eruption Times Series 1

Date	Direct Radiation [Wm^{-2}]
1982.39	347.03
1982.48	369.17
1982.56	384.44
1982.68	407.35
1982.82	439.42
1983.48	12.00
1983.60	488.30
1983.91	499.76
1984.63	506.66
1985.61	518.91
1986.36	521.23
1987.16	526.60
1988.53	64.00
1988.71	527.43
1990.38	525.96
1991.07	529.81

Table 8: Eruption Times Series 2

Date	Direct Radiation [Wm^{-2}]
1991.67	390.14
1991.87	412.28
1992.19	439.77
1992.45	464.21
1993.14	502.41
1993.83	516.94
1994.69	523.84
1995.72	527.69
1996.96	530.80
1998.05	532.36
1998.45	531.62

5.3.2 Parameters

Table 9: Zonal Parameters

	Parameter	Value
Zone 1	Geometric Factor, γ_1	0.1076
	Area Fraction, A_1	0.067
	Land Fraction, f_1^s	0.0
	Ocean Fraction, f_1^w	0.550925926
	Ice Fraction, f_1^i	0.449074074
Zone 2	Geometric Factor, γ_2	0.2277
	Area Fraction, A_2	0.183
	Land Fraction, f_2^s	0.074074074
	Ocean Fraction, f_2^w	0.925925926
	Ice Fraction, f_2^i	0.0
Zone 3	Geometric Factor, γ_3	0.3045
	Area Fraction, A_3	0.25
	Land Fraction, f_3^s	0.240740741
	Ocean Fraction, f_3^w	0.759259259
	Ice Fraction, f_3^i	0.0
Zone 4	Geometric Factor, γ_4	0.3045
	Area Fraction, A_4	0.25
	Land Fraction, f_4^s	0.3101851851
	Ocean Fraction, f_4^w	0.689814815
	Ice Fraction, f_4^i	0.0
Zone 5	Geometric Factor, γ_5	0.2277
	Area Fraction, A_5	0.183
	Land Fraction, f_5^s	0.694444444
	Ocean Fraction, f_5^w	0.305555556
	Ice Fraction, f_5^i	0.0
Zone 6	Geometric Factor, γ_6	0.1076
	Area Fraction, A_6	0.067
	Land Fraction, f_6^s	0.277777778
	Ocean Fraction, f_6^w	0.652777778
	Ice Fraction, f_6^i	0.069444444

Table 10: Global Parameters

Parameter	Value	Units
Stefan-Boltzmann Constant, σ_B	5.6696e-8	$Wm^{-2}K^{-4}$
Solar Constant, S_0	1368	Wm^{-2}
Earth Radius, R_E	6371e3	m
Earth Total Emissivity, ϵ	1	
Surface Area of Earth, A_E	πR_E^2	m^2
Atmospheric Transmissivity, τ	0.63	
Atmospheric Albedo, α_{sky}	0.2	
Land Albedo, α_s	0.4	
Ocean Albedo, α_w	0.1	
Ice Albedo, α_i	0.6	
Land Density, ρ_s	2500	kgm^{-3}
Ocean Density, ρ_w	1028	kgm^{-3}
Ice Density, ρ_i	900	kgm^{-3}
Land Thermal Scale Depth, $[Z_s]$	1.0	m
Ocean Thermal Scale Depth, $[Z_w]$	70.0	m
Ice Thermal Scale Depth, $[Z_i]$	1.0	m
Land Specific Heat Capacity, c_s	790	$JkgK^{-1}$
Ocean Specific Heat Capacity, c_w	4187	$JkgK^{-1}$
Ice Specific Heat Capacity, c_i	2060	$JkgK^{-1}$

Table 11: Boundary Parameters

Parameter	Value	Units
Boundary 12 ($60°S$)		
Boundary Length, L_{12}	2.0015e7	m
Thermal exchange coefficient, k_{12}	1e7	$Wm^{-1}K^{-1}$
Boundary 23 ($30°S$)		
Boundary Length, L_{23}	3.4667e7	m
Thermal exchange coefficient, k_{23}	1e7	$Wm^{-1}K^{-1}$
Boundary 34 ($0°S$)		
Boundary Length, L_{34}	4.0030e7	m
Thermal exchange coefficient, k_{34}	1e7	$Wm^{-1}K^{-1}$
Boundary 45 ($30°N$)		
Boundary Length, L_{45}	3.4667e7	m
Thermal exchange coefficient, k_{45}	5e7	$Wm^{-1}K^{-1}$
Boundary 56 ($60°N$)		
Boundary Length, L_{56}	2.0015e7	m
Thermal exchange coefficient, k_{56}	1e7	$Wm^{-1}K^{-1}$

References

Budyko, M. (Dec. 1969). "The effect of solar radiation variations on the climate of Earth". In: *Tellus* 21, 5, pp. 611–619. URL: https://doi.org/10.3402/tellusa.v21i5.10109.

Jellinek, M. (Nov. 2020). "Volcanic Eruptions and Climate Change". In: *EOSC 453* At: University of British Columbia, Vancouver, Canada.

Robock, A. (May 2000). "Volcanic eruptions and climate". In: *Reviews of Geophysics* 38, 2, pp. 191–219.